nature communications

Article

https://doi.org/10.1038/s41467-025-57847-x

SSUP-72/PINN-1 coordinates RNA-polymerase II 3′ pausing and developmental gene expression in *C. elegans*

Received: 26 May 2024

Accepted: 5 March 2025

Published online: 17 March 2025

Check for updates

François-Xavier Stubbe[1], Pauline Ponsard[1], Florian A. Steiner[2] & Damien Hermand[1,3]

During exit from *Caenorhabditis elegans* (C. elegans) L1 developmental arrest, a network of growth- and developmental genes is activated, many of which are organized into operons where transcriptional termination is uncoupled from mRNA 3′-end processing. CDK-12-mediated Pol II CTD S2 phosphorylation enhances SL2 trans-splicing at downstream operonic genes, preventing premature termination and ensuring proper gene expression for developmental progression. Using a genetic screen, we identified the SSUP-72/PINN-1 module as a suppressor of defects induced by CDK-12 inhibition. Loss of SSUP-72/PINN-1 bypasses the requirement for CDK-12 in post-embryonic development. Genome-wide analyses reveal that SSUP-72, a CTD S5P phosphatase, affects Pol II 3′ pausing and regulates intra-operon termination. Our findings establish SSUP-72/PINN-1 as a key regulator of Pol II dynamics, coordinating operonic gene expression and growth during *C. elegans* post-embryonic development.

Transcription generates gene expression patterns that allow cells to perform specialized roles within an organism, to adapt to a changing environment, and to maintain basic metabolic processes. Protein-coding genes are transcribed by the RNA polymerase II (Pol II). The largest subunit of Pol II harbors an unstructured tail-like C-terminal domain (CTD) composed of repeats of the consensus heptapeptide sequence Y-S-P-T-S-P-S[1–3]. This CTD functions as a phase-separated dynamic surface for recruiting proteins required for co-transcriptional mRNA processing or the interaction with specific histone modifications[4,5].

Pol II is recruited to transcription units (TU) with a hypo-phosphorylated CTD that becomes heavily phosphorylated on serine 5 (CTD S5P) during the transition from initiation to early elongation, and then on serine 2 (CTD S2P) during productive elongation, generating a dual gradient, which temporally and functionally couples transcription and mRNA processing[6–10]. In yeast, the only essential function of CTD S5P is to ensure the timely recruitment of the capping machinery to the nascent transcript[11], and it is assumed that CTD S2P plays a similar role in recruiting factors for splicing and mRNA 3′ end formation. Indeed, CTD S2P enhances the recruitment of the Cleavage a Polyadenylation Specificity Factor and Cleavage and Stimulatory Factor complexes (CstF), which are essential for cleavage, polyadenylation, and transcription termination[12,13]. Termination is coupled to 3′ end processing since the free 5′ end resulting from the cleavage is targeted by the nuclear exoribonuclease Rat1/Xrn2, which acts as a "torpedo" to remove Pol II from the chromatin template[14]. However, while the 3′ end machinery is essential in both fission and budding yeast, CTD S2P is not[15]. Therefore, the dependency on CTD S2P for 3′ end processing appears to be weak. The Cdk12 kinase is responsible for the bulk of CTD S2P and accordingly is not essential in fission or budding yeast[16,17].

In *C. elegans*, inhibition or knock-down of CDK-12 leads to the loss of CTD S2P and causes a reversible L1 (first larval stage) developmental arrest, mimicking all the features of the developmental diapause observed when embryos hatch in the absence of food[18]. At the level of transcription, CDK-12 is mainly required for the expression of the growth- and development-related genes located at position 2 or downstream within operons. Operons are clusters of 2–8 genes under the control of a single promoter[19]. Operons are enriched for housekeeping genes required for growth and development[20] and were

[1]URPHYM-GEMO, The University of Namur, Namur, Belgium. [2]Department of Molecular and Cellular Biology, Faculty of Sciences, University of Geneva, Geneva, Switzerland. [3]The Francis Crick Institute, London, UK. e-mail: Damien.Hermand@crick.ac.uk

proposed to be an adaptation to limit the transcriptional resources required to induce this large set of genes simultaneously[21]. A single polycistronic pre-mRNA is converted co-transcriptionally into multiple mature monocistronic mRNAs, where the 5′-ends are formed by *trans-splicing* of a cap-like 22-nucleotide splice leader (SL). The genes in position 1 are *trans-spliced* to a SL1, whereas genes in position 2 and over are *trans-spliced* to a SL2[22]. SL2 *trans-splicing* is associated with the polyadenylation of the upstream mRNA and prevents transcription termination. The SL2 particle is recruited by the CstF complex[23], which itself requires high CTD S2P levels, thus explaining the requirement of CDK-12 for SL2 *trans-splicing*. Even when proper termination is absent, CTD S2P peaks on operonic loci's 3′ ends. This unique uncoupling between CTD S2P and transcription termination is well-suited for the dissection and understanding of these processes.

To better understand the role of CDK-12 and CTD S2P during early post-embryogenesis development and to identify additional regulators of SL2 *trans-splicing*, we conducted a forward genetic screen. We identified a mutation in the *ssup-72* gene that encodes a CTD S5P phosphatase[24–26] as an efficient suppressor of the L1 arrest induced by CDK-12 inhibition. Further analyses revealed that the SSUP-72/PINN-1 module[27] is required for Pol II 3′ pausing genome-wide to coordinate the expression of growth and developmental genes in *C. elegans*.

Results

SSUP-72 suppresses the L1 arrest from CDK-12 inhibition

cdk-12 lesions in *C. elegans* induce a fully penetrant early post-embryogenic developmental arrest that we refer to as "L1 arrest". To identify mutations that allow animals to bypass this arrest, we mutagenized *cdk-12AS* (an analogue-sensitive version of CDK-12) worms with ethyl methanesulfonate (EMS) and subjected their F2 offspring to 3MB-PP1 inhibition. We recovered five worm lines that developed normally when CDK-12 activity was inhibited. Whole genome sequencing revealed that one of the suppressors carried a mutation in the *ssup-72* gene, resulting in a glutamic acid to lysine substitution at position 22 (E22K, Fig. 1A). We recreated the mutation by CRISPR-Cas9 gene editing in the *cdk-12as* background and confirmed that *ssup-72[E22K]* bypasses the L1 arrest caused by CDK-12as inhibition (Fig. 1B). To further validate this finding, we crossed a *ssup-72* null allele (*tm2304*) into *CDK-12AS* worms, which confirmed that the loss of SSUP-72 suppresses the requirement of CDK-12 for early larval development (Fig. 1C).

Because CDK-12 is responsible for the bulk of Pol II CTD S2 phosphorylation (CTD S2P), we asked whether the *ssup-72[E22K]* allele also restores wild-type levels of CTD S2P. L1-synchronized worms cultured for 4 h in the presence of 3MB-PP1 (2 μM) were lysed and analyzed by western blot, which showed that the suppression occurs independently of CTD S2P levels (Fig. 1D and Supplementary Fig. 2A). This uncoupling of CTD S2P levels and the larval growth phenotype led us to test if the *ssup-72[E22K]* allele could also suppress the defects resulting from the inhibition of CDK-9, the second elongation-specific CTD kinase. We generated an analogue-sensitive *cdk-9[M171G]* version using CRISPR-Cas9 gene editing. Confirming previous RNAi analyses[28], the inhibition of CDK-9as resulted in penetrant embryonic lethality and developmental delays, neither being rescued by the *ssup-72[E22K]* allele (Supplementary Fig. 1A, B). These data indicate that the *ssup-72[E22K]* allele specifically suppresses the requirement of CDK-12 for early larval development. Interestingly, the suppression by *ssup-72[E22K]* is dose-dependent. Increasing the dose of the inhibitor and, therefore, decreasing the level of CDK-12 activity gradually weakens the suppression by *ssup-72[E22K]* (Fig. 1E). Consistently, the *ssup-72[E22K]* allele does not suppress the L1 arrest caused by a *cdk-12(tm3864)* null allele. However, the *ssup-72(tm2304)* null allele suppresses the early developmental arrest in *cdk-12(tm3864)* homozygous worms. These results imply that *ssup-72[E22K]* is a hypomorphic allele rather than a complete loss of function allele.

Together with our previous work on the role of CDK-12 in operon transcription[18], our results suggest that CDK-12 and SSUP-72 collaborate to regulate the expression of operonic genes.

Increased CTD-S5P bypasses CDK-12 in exit from L1 arrest

While SSUP-72 has previously been associated with the mRNA 3′ end processing machinery[26], its role in this process remains elusive, and it is unclear why the *SSU72* gene is essential in budding yeast but dispensable in other species, including fission yeast and *C. elegans*. Because the *ssup-72* null mutant allele suppresses the inhibition of CDK-12as similarly to the *ssup-72[E22K]* allele (Fig. 1C), we wondered if the suppression solely requires the loss of the catalytic activity of SSUP-72, or if it is mediated through structural effects resulting from of the absence of the protein.

The catalytic pocket of the SSU72 family contains a well-studied and typical CX_5R motif, where a Cysteine to Serine substitution abolishes its CTD S5P phosphatase activity[25]. We generated a phosphatase-dead *ssup-72[C13S]* allele and found that the *cdk-12as;ssup-72[C13S]* strain does not arrest its development upon CDK-12as inhibition (Fig. 1F). To support this finding, we tested previously reported mutations at serine 39 (S39), the phosphorylation of which was shown to downregulate SSUP-72 activity in *C. elegans*[29]. A phosphomimetic *ssup-72[S39E]* allele suppressed CDK-12 inhibition while the non-phosphorylable *ssup-72[S39A]* allele did not (Supplementary Fig. 1C). Together, these data suggest that various ways of experimentally downregulating either SSUP-72 levels or phosphatase activity all result in the suppression of CDK-12as inhibition and a rescue of the L1 arrest.

While SSUP-72 has mainly been described as a CTD S5P phosphatase, it also has CTD-independent substrates associated with physiological functions and pathogenesis[30–32]. Previous biochemical studies have unveiled that SSUP-72 specifically binds to CTD repeats harboring a Proline 6 (P6) in the *cis* conformation, because the phosphatase catalytic site is enclosed in a narrow groove formed by two β-sheets, which restrains CTD conformation accessibility[33]. Therefore, the *peptidyl-prolyl-cis-trans* isomerase PINN-1 that catalyzes the CTD P6 *cis-trans* isomerization is required for the binding of SSUP-72 to the CTD and for CTD S5P dephosphorylation[34]. In addition, *Ssu72* and *Pin1* form a functional module within the 3′ processing machinery[27,33]. We found that a *pinn-1* null allele (*tm2235*) rescued CDK-12as inhibition (Fig. 1F), strengthening the hypothesis that keeping SSUP-72 activity away from the CTD results in the suppression of CDK-12as inhibition.

Next, we used quantitative western blotting with synchronized L1 larvae fed for 4 h before protein extraction to determine the levels of CTD S5P. We observed ~35% higher levels in bulk CTD S5P level in the *pinn-1* and *ssup-72* null mutants compared to the wild type (Fig. 1G and Supplementary Fig. 2B). The catalytic-dead *ssup-72[C13S]* and the screening-recovered *ssup-72[E22K]* mutants showed similarly increased CTD S5P levels (Fig. 1G).

CDK-12 regulates transcription elongation

To better understand the effect of CDK-12as inhibition on transcription at a genome-wide level, we adapted Global run-on sequencing (GRO-seq) to L1 nuclei. Compared to ChIP-seq or RNA-seq, GRO-seq has the advantage of measuring nascent RNA. Worms were synchronized at the L1 stage and cultured in the presence or absence of 3MB-PP1 (2 μM) for 4 h before isolating nuclei and performing the nuclear run-on. The GRO-seq data were used to generate rescaled metagene plots showing Pol II density for all non-operonic *C. elegans* protein-coding genes (Fig. 2A, left panel). In contrast to humans[35], worm Pol II only slightly pauses at 5′ ends but undergoes extensive pausing towards the 3′ ends, likely allowing 3′ RNA processing[36]. The inhibition of CDK-12as in worms results in an altered distribution of Pol II occupancy over active genes, characterized by an overall increase of Pol II occupancy (Fig. 2A, left panel). The increased gene body occupancy is consistent with impaired Pol II elongation progression or less processive (slower) Pol

https://doi.org/10.1038/s41467-025-57847-x

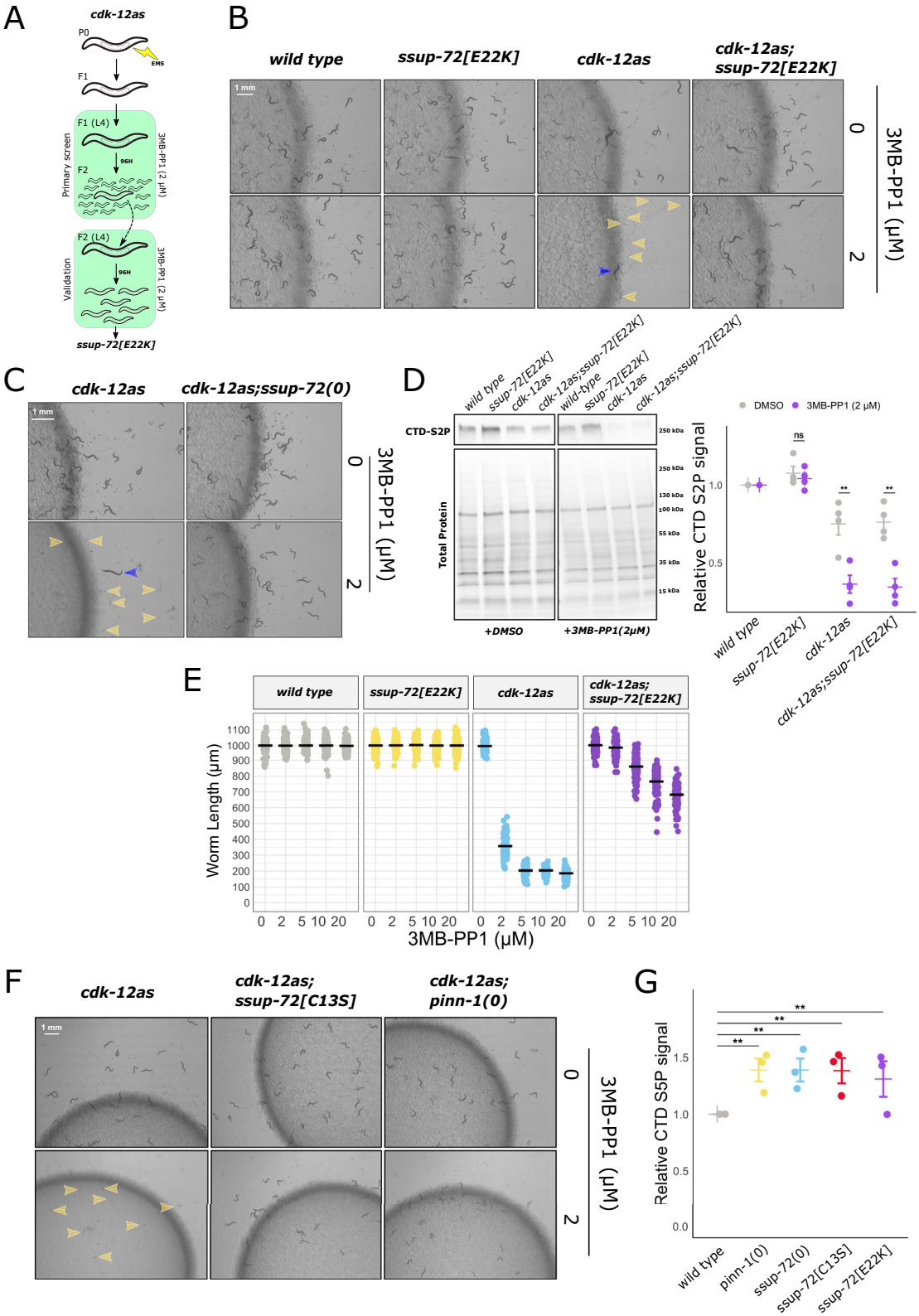

II. We computed a "processivity score" (defined as the ratio of Pol II occupancy at the 3′ end of the gene over the 5′ end of the gene) to quantify this change in individual genes, confirming a global elongation defect in *cdk-12as* worms. (Fig. 2B, C). Very unexpectedly, the Pol II profile was nearly identical in the *cdk-12as* stain that arrests at L1 and the *cdk-12as;ssup-72[E22K]* strain that grows like the wild type, indicating that the effect of CDK-12as inhibition on transcriptional elongation is very unlikely to cause the L1 developmental arrest directly. The GRO-seq experiment also revealed that while the SSUP-72[E22K] mutation does not affect transcription during initiation and elongation, it globally decreases 3′ pausing (Fig. 2A, right panel), which supports a specific role of CTD S5P dephosphorylation in this process. Notably, this decreased pausing occurs without any distinctive effect on worm growth or development in the *ssup-72* mutants.

https://doi.org/10.1038/s41467-025-57847-x

Fig. 1 | Mutations of the SSUP-72/PINN-1 module suppress the developmental arrest resulting from inhibition of CDK-12as. A Schematic overview of the EMS mutagenesis and screen for suppressors of the L1 developmental arrest resulting from the inhibition of the CDK-12as (analogue-sensitive) mutant. **B**, **C** Transmitted light images of the indicated strains and conditions. Images were taken 96 h after depositing individual P0 worms at L4 stage. Blue arrows point to the P0, yellow arrows to L1 arrested worms. **D** Left, Western blot analysis of Pol II CTD-S2P levels at L1 stage in the indicated strains and conditions. Uncropped scan in Supplementary Fig. 2A. Right, quantification of CTD S2P intensities normalized to total protein signal. The intensities for the wild type were set to 1. Significance was tested using a two-tailed unpaired *t*-test test (ns not significant, ** = <0.01). Measurements were taken from 3 independent replicates. Error bars represent standard deviation. **E** Worm length as a proxy for growth, measured after 72 h of CDK-12as inhibition, starting with staged L1 worms of the indicated strains and conditions. Measurements were taken from two independent replicates. **F** Transmitted light images of the indicated strains and conditions. Images were taken 96 h after depositing individual P0 worms at L4 stage. **G** Quantification of Western blot analysis of CTD S5P levels normalized to total protein in L1-staged worms from the indicated strains. The intensities for the wild type were set to 1. Significance was tested using a two-tailed unpaired *t*-test (** = <0.01). Measurements were taken from three independent replicates. Error bars represent standard deviation. Error bars represent standard deviation.

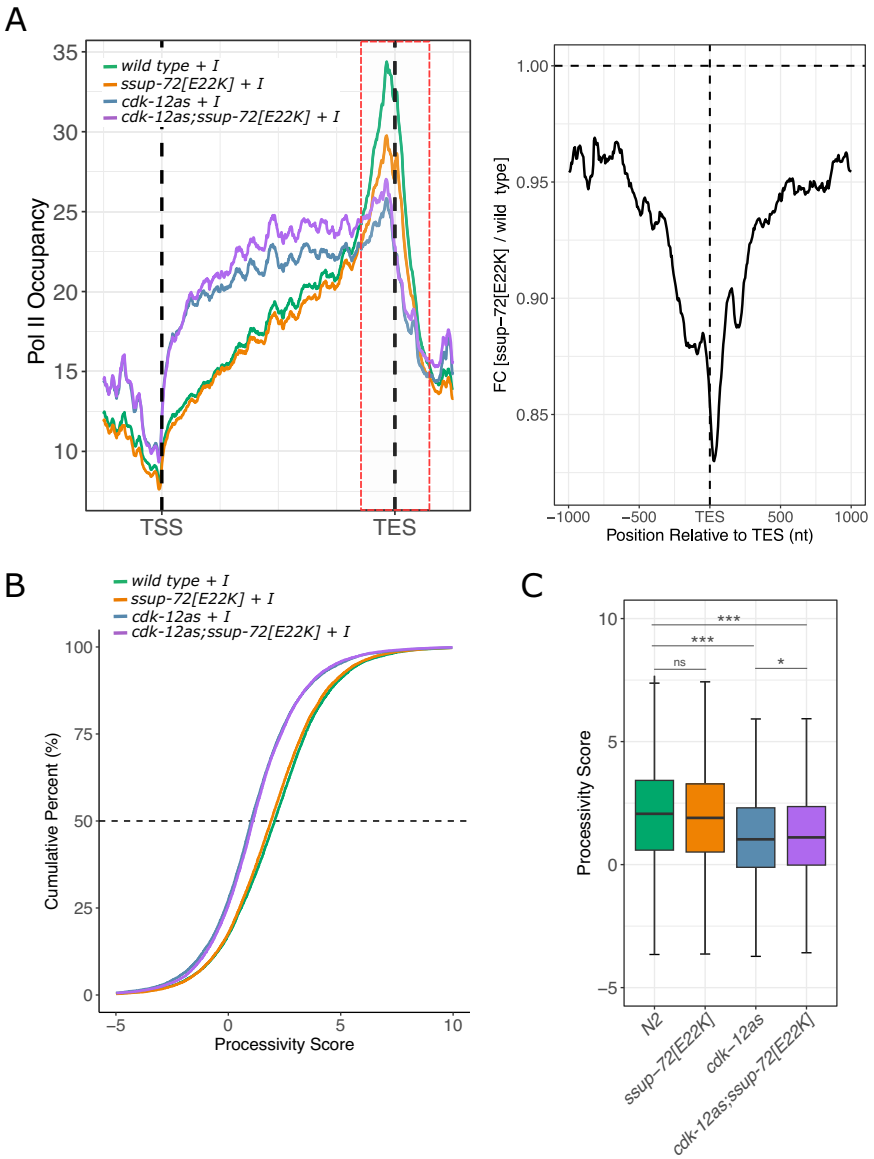

Fig. 2 | The phosphatase SSUP-72 is required for efficient pausing of Pol II at the 3′ end. A Left panel: Metagene analysis of GRO-seq signal at non-operonic protein-coding genes ($n = 16411$). The GRO-seq signal was averaged for all genes and aligned at their annotated transcription start site (TSS) and transcription end site (TES) for the indicated strains and conditions. +I denotes growth in the presence of 2 μM 3MB-PP1. The plot was generated using data from three replicates. The red box highlights the 3′ end region where pausing defects are observed. Right panel: Ratio of GRO-seq signal from *ssup-72[E22K]* over wild type, aligned at the TES, highlighting the lower Pol II density at the 3′ end in the *ssup-72[E22K]* single mutant compared to the wild type. **B** Empirical cumulative distribution plots of the processivity score on individual genes in the indicated strains and conditions, as in (**A**). The plot was generated from three replicates of GRO-seq data. **C** Boxplot showing processivity scores for all isolated protein-coding genes, in the indicated strains and conditions. Worms were grown in the presence of 2 μM 3MB-PP1. Significance was tested using a two-tailed Mann–Whitney–Wilcoxon test (ns not significant, * = <0.05, *** = <0.001). The plot was generated from three replicates of GRO-seq data. Boxplots display median (line), first, and third quartiles (box), and 90th/10th percentile values (whiskers).

https://doi.org/10.1038/s41467-025-57847-x

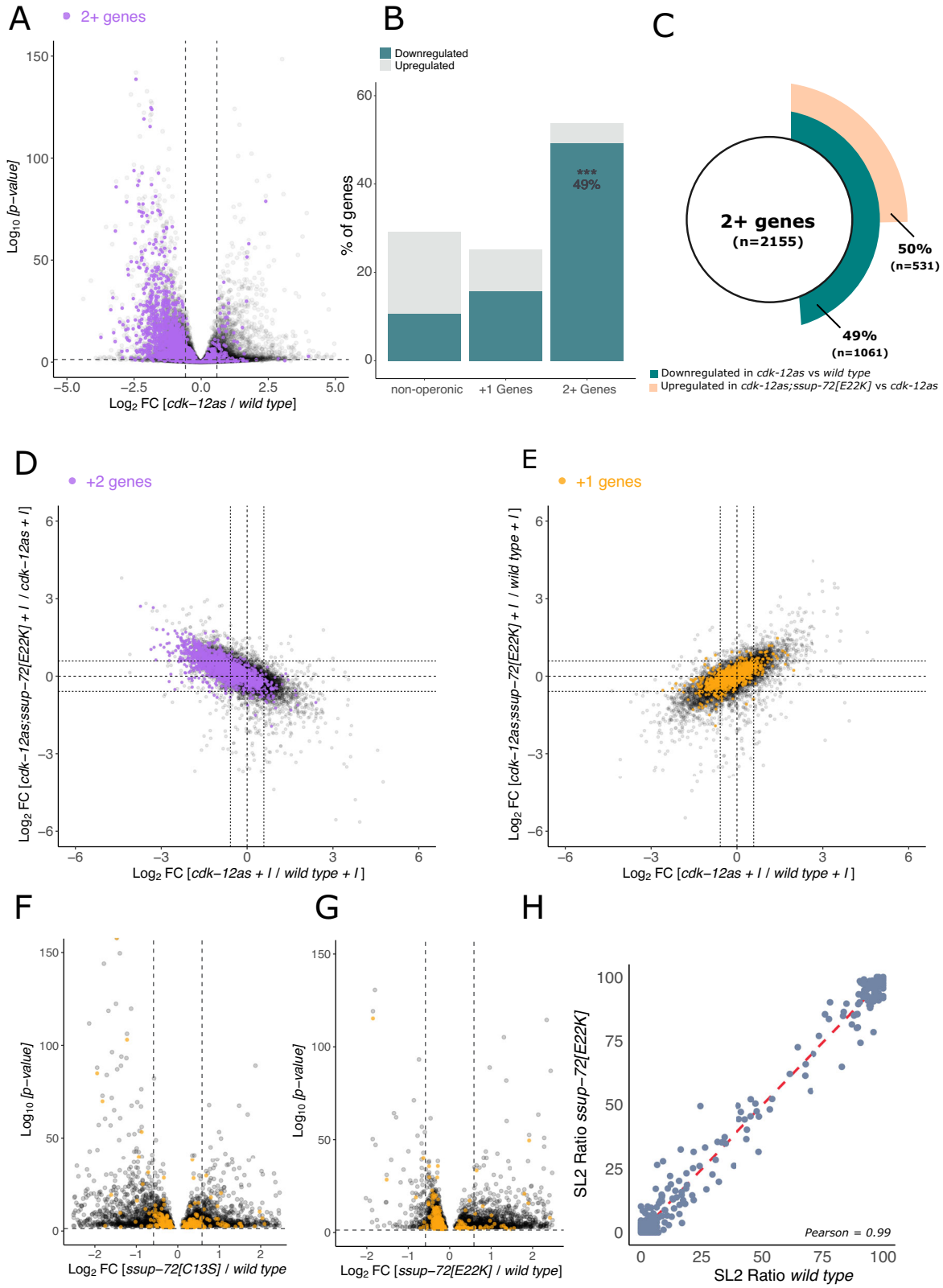

SSUP-72 loss restores SL2 *trans-splicing* after CDK-12 inhibition

In *C. elegans*, the loss of CDK-12 results in decreased levels of mRNAs from genes located in position two and over (2+ genes) within operons (Fig. 3A, B), which results from their inefficient *trans-splicing* and increased torpedo transcription termination. To test if the suppression by the *ssup-72[E22K]* allele was associated with restored levels of mRNAs transcribed from 2+ genes, we conducted RNA-seq experiments. We found this to be partially the case, with 50% of 2+ genes downregulated upon CDK-12as inhibition being significantly upregulated in the *cdk-12as;ssup-72[E22K]* strain compared to the *cdk-12as* strain (Fig. 3C, D). However, the mRNA levels of 2+ genes in the *cdk-12as;ssup-72[E22K]* strain were still lower than in the wild type (Supplementary Fig. 3).

Fig. 3 | The downregulation of SSUP-72 restores efficient expression of SL2 *trans-spliced* mRNAs that are downregulated upon CDK-12 inhibition. **A** Volcano plot showing *cdk-12as*-dependent changes in transcript levels as determined by RNA-seq (CDK-12as inhibited compared to the wild-type). +I denotes growth in the presence of 2 μM 3MB-PP1. Purple dots highlight 2+ encoded mRNAs within operons ($n = 2155$). The dotted lines indicate a Fold Change of ±1.5 (vertical) and a p-value < 0.05 (horizontal) (Wald test). The plot was generated from 3 independent replicates. **B** Bar graphs showing the relative percentage of *cdk-12as*-dependent changes (RNA-seq) by the operonic position (non-operonic: isolated genes, $n = 16411$; +1 Genes: First position genes within operons, $n = 1430$; 2+ Genes: Genes at position 2 and over within operons, $n = 2155$). *Chi-square* statistical test (*** = *p-value* < 0.001). The plot was generated from 3 independent replicates. **C** Schematic of the suppression of the 2+ gene downregulation in *cdk-12as;ssup-72[E22K]* compared to *cdk-12as*. The proportion of 2+ genes that is downregulated in *cdk-12as* worms compared to wild type is shown in green. The proportion of 2+ genes affected by the inhibition of CDK-12as that is upregulated in *cdk-12as;ssup-72[E22K]* compared to *cdk-12as* is shown in orange. **D** Comparison between mRNA *cdk-12as*-dependent changes in mRNA levels (*x*-axis: *cdk-12as*/wild-type) and the *cdk-12as;ssup-72[E22K]* suppressive changes (*y*-axis: *cdk-12as;ssup-7[E22K]*/*cdk-12as*) (RNA-seq). +I denotes growth in the presence of 2 μM 3MB-PP1. 2+ genes ($n = 2155$) are highlighted with purple dots. The dotted lines indicate a Fold Change of ±1.5. The plot was generated from three independent replicates. **E** Comparison between *cdk-12as*-dependent changes in mRNA levels (*x*-axis: *cdk-12as*/wild-type) and the *cdk-12as;ssup-72[E22K]*-dependent changes (*y*-axis: *cdk-12as;ssup-7[E22K]*/*wild-type*) (RNA-seq). +I denotes growth in the presence of 2 μM 3MB-PP1. +1 genes ($n = 1430$) are highlighted with orange dots. The dotted lines indicate a Fold Change of ±1.5. The plot was generated from three independent replicates. **F**, **G** Volcano plots showing *ssup-72*-dependent changes (**F**: *ssup-72[C13S]*, **G**: *ssup-72[E22K]*) in transcript levels as determined by RNA-seq. +1 genes ($n = 1430$) are highlighted with orange dots. The dotted lines indicate a Fold Change of ±1.5 (vertical) and a p-value < 0.05 (horizontal) (Wald test). The plot was generated from three independent replicates. **H** Correlation between the SL2 score (SL2/SL2 + SL1) in *ssup-72[E22K]* mutant and the wild type. The red dotted line is the linear regression. Only genes with at least 10 matching splice-leader reads were kept for the analysis ($n = 1739$).

To clarify if the suppression of the L1 arrest observed in the *cdk-12as;ssup-72[E22K]* results from a global increase in operonic transcription, we analyzed the RNA-seq levels of the genes in first position (+1 genes) within operons. If operons are more heavily transcribed, +1 genes would be upregulated in *ssup-72* mutants compared to the wild type. Unlike 2+ genes, +1 genes are barely affected in *cdk-12as*, and behave similarly in *cdk-12as;ssup-72[E22K]*, without any obvious trend (Fig. 3E). Similarly, we found that +1 gene expression is not increased in the *ssup-72[C13S]* nor *ssup-72[E22K]* mutants (Fig. 3F, G). A possible explanation for the stabilization of 2+ genes, which are SL2 *trans-spliced*, would be a swap from SL2 to SL1 *trans-splicing*. We used SL-quant[37] to compute the SL2 ratio, which is defined as the ratio of SL2 to SL1 containing reads for each gene. The *ssup-72[E22K]* strain displays a very strong correlation (pearson >0.99) in SL usage with the wild type (Fig. 3H). This indicates that the suppression by the *ssup-72[E22K]* mutation is not mediated by replacing the SL2 *trans-splicing* of 2+ genes with SL1 *trans-splicing*.

SSUP-72 controls early termination within operons

To better understand the effect of CDK-12 and SSUP-72 on operonic Pol II dynamics, we leveraged the GRO-seq data and generated rescaled metagene plots of Pol II occupancies for both +1 genes and 2+ genes (Fig. 4A). +1 genes have a similar profile to non-operonic protein-coding genes (Fig. 2A), with increased Pol II occupancy over the gene body in both the *cdk-12as* and the *cdk-12as;ssup-72[E22K]* strains compared to the wild type. In contrast, 2+ genes show a higher Pol II occupancy in the *cdk-12as;ssup-72[E22K]* strain compared to the *cdk-12as* strain (Fig. 4A). This increased Pol II occupancy in the suppressor strain, which is comparable to the wild type, likely explains both the restored 2+ mRNA levels and the rescue of the L1 developmental arrest.

We previously reported that the inactivation of CDK-12 causes SL2 *trans-splicing* failure and increased torpedo termination at 2+ genes[18]. Accordingly, GRO-seq revealed a gradual decrease of Pol II occupancy from the first to the second to the third gene of the operons when CDK-12as is inhibited (Fig. 4B, top panel). The presence or the *ssup-72[E22K]* mutation in the *cdk-12as;ssup-72[E22K]* strain reversed this tendency, resulting in increased occupancy on 2+ genes and increased Pol II retention immediately next to the TES compared to the *cdk-12as* strain (Fig. 4B, bottom panel). In line with this result, GRO-seq signal on 2+ genes in the *cdk-12as;ssup-72[E22K]* strain is near wild-type (Supplementary Fig. 4).

These data indicate that the loss of SSUP-72 phosphatase activity counteracts the early transcription termination by Pol II at 2+ genes that occurs when CDK-12as is inhibited, thereby providing a molecular mechanism for the suppression. We next asked whether this effect also occurs in non-operonic genes. We did not see an accumulation of GRO-seq signal downstream of the TES (Fig. 4C and Supplementary Fig. 5), which indicates that Pol II is not retained beyond non-operonic TES. We therefore concluded that the increased Pol II retention is specific to 2+ genes.

SSUP-72 coordinates operonic developmental gene expression

SSUP-72 was previously implicated in stimulating termination at an early polyadenylation signal (PAS) in the ankyrin gene *unc-44*[29]. This gene expresses a short isoform (*unc-44c*) and a long isoform (*unc-44f*). Expression of *unc-44f* requires the inactivation of SSUP-72 by phosphorylation of S39, which allows for bypass termination at the early PAS and to express the long isoform. To investigate whether the various mutants we generated within the SSUP-72/PINN-1 module dampen transcription termination at the early PAS of *unc-44*, we compared the normalized RNA-seq reads from these mutants to the wild type across the *unc-44* locus. While strains containing the *pinn-1(0), ssup-72(0), and ssup-72[C13S]* alleles show increased levels of the long *unc-44f* mRNA, only a moderate increase is observed in the strain with the screen-recovered *ssup-72[E22K]* allele (Supplementary Fig. 6). In addition, the strain with the phosphomimetic *ssup-72[S39E]* allele (inactive form) expresses the *unc-44f* isoform, while the strain with the non-phosphorylatable *ssup-72[S39A]* variant (active form) expresses it less than the wild type. However, none of these *ssup-72* mutants displays a changed RNA-seq signature on operons (Supplementary Fig. 7).

These data show that while the genome-wide decreased Pol II pausing at the TES resulting from SSUP-72 inactivation does not result in a global termination defect (Fig. 2A), in the specific case of *unc-44*, it has a strong effect on bypassing termination at the early PAS (Supplementary Fig. 6). This effect likely requires the complete inactivation of SSUP-72 by S39 phosphorylation, because the E22K mutant that retains some activity (Fig. 1G) only modestly affects the expression of the long *unc-44f* mRNA.

To extend the analysis of how SSUP-72 impacts 3′ pausing and termination at various classes of genes, we used the GRO-seq data to map the occupancy of active Pol II around all TES of protein-coding genes in the presence or absence of SSUP-72 activity. Regardless of where the TES is located (non-operonic genes, +1 genes, or 2+ genes) we observed a drop in the GRO-seq signal at the TES (Fig. 4C), confirming that the reduced 3′ end pausing of Pol II is resulting from the downregulation of SSUP-72 (Fig. 2A).

A plausible consequence of the decreased Pol II 3′ end pausing observed when SSUP-72 is inactivated is an altered pre-mRNA cleavage efficiency and/or dynamic. If this is the case, the intergenic region between operonic genes (referred to as SL2 outrons) (Fig. 4B) should be detected at higher levels. We indeed observe such an increase in SL2 outrons in the RNA-seq data for the phosphomimetic *ssup-72[S39E]*

https://doi.org/10.1038/s41467-025-57847-x

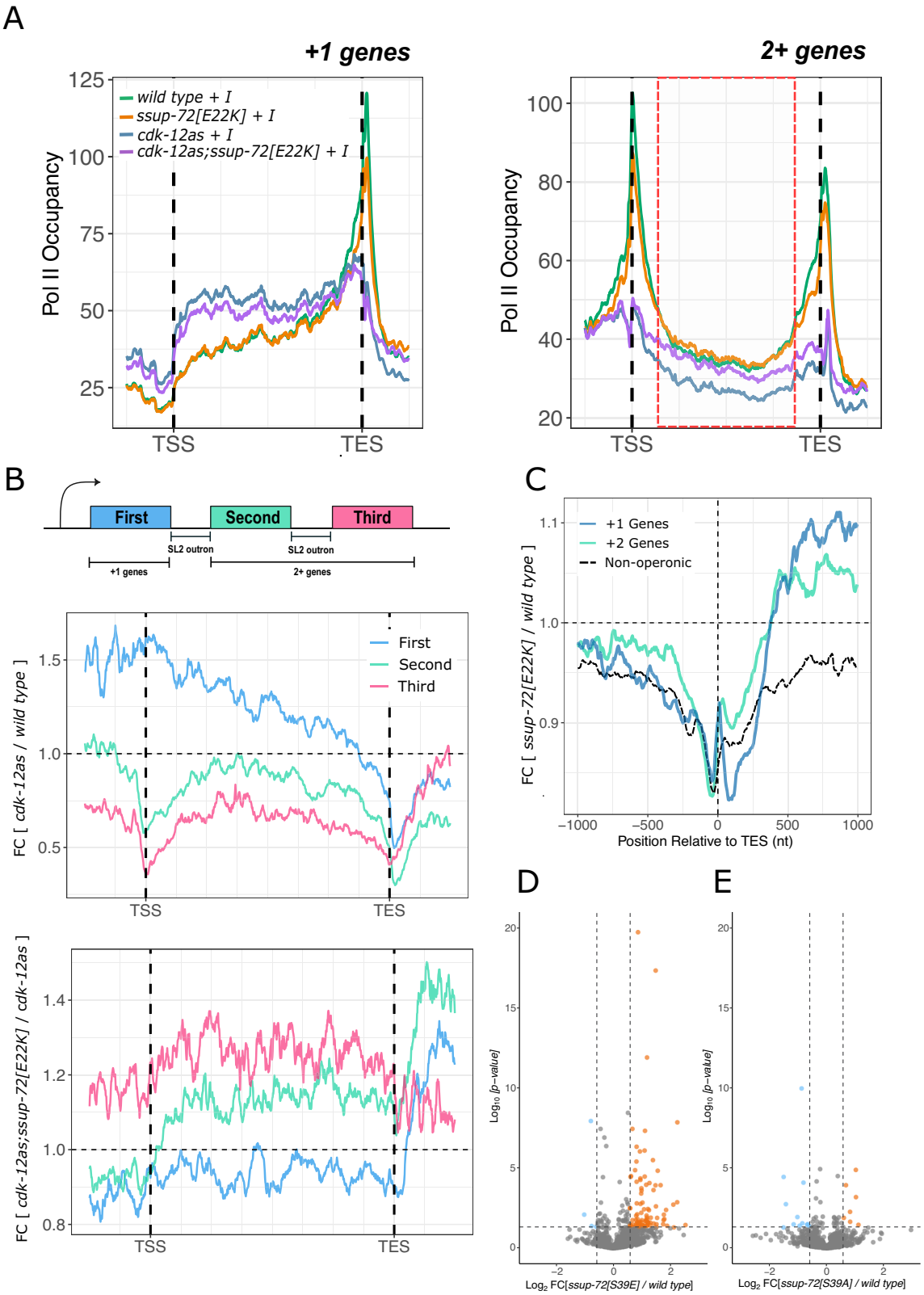

mutant (Fig. 4D). In contrast, the non-phosphorylatable *ssup-72[S39A]* allele, which does not suppress the L1 arrest, did not alter the levels SL2 outrons (Fig. 4E).

These data reveal a role for SSUP-72 in regulating Pol II pausing between operonic genes for the coordinated expression of developmental genes arranged in operons.

Discussion

Lesions in *CDK-12* in *C. elegans* induce a fully penetrant yet reversible early larval (L1) arrest, mimicking a developmental diapause. This L1 arrest is due to the loss of operonic SL2 *trans-spliced* mRNAs encoding proteins required for growth and development[18]. To better understand how the developmental arrest is regulated, we conducted a suppressor

Fig. 4 | The downregulation of SSUP-72 inhibits premature Pol II transcription termination at position 2 and over within operons. A Left panel: Metagene analysis of GRO-seq signal for the first genes (+1 genes) within operons ($n = 1430$) in the indicated strains and conditions. +I denotes growth in the presence of 2 μM 3MB-PP1. Right panel: Metagene analysis of GRO-seq signal for the 2+ genes within operons ($n = 2155$). The red box highlights the gene bodies showing the restoration of a wild-type level of Pol II occupancy during elongation in the *cdk-12as;ssup-72[E22K]* strain. The plots were generated using data from three replicates. The GRO-seq signal was averaged and aligned at the annotated transcript start sites (TSS) and transcript end sites (TES). **B**. Top panel: schematic of a three genes operon structure showing the genes and outrons. Middle panel: Metagene fold change analysis of *cdk-12as* over wild-type GRO-seq signal. Bottom panel: Metagene fold change analysis of *cdk-12as;ssup-72[E22K]* over *cdk-12as* GRO-seq signal. Only operons harboring three genes ($n = 296$) were considered. The metagene plots were generated using data from three replicates. The GRO-seq signal was averaged and aligned at the annotated transcript start sites (TSS) and transcript end sites (TES). **C** Metagene Analysis of *ssup-72[E22K]* over wild-type (N2) GRO-seq signal aligned around annotated transcript end sites (TES). Non-operonic genes ($n = 16411$), first genes within operons ($n = 1430$), 2+ genes within operons ($n = 2155$). The plots were generated from three independent replicates. **D**, **E** Volcano plots showing the differential expression of SL2 outrons ($n = 1621$) in *ssup-72* mutants (**D**: *ssup-72[S39E]*, **E**: *ssup-72[S39A]*) compared to the wild type. Orange dots highlight significantly increased outron detection, and blue dots highlight significantly decreased outron detection. The dotted lines indicate a fold change of ±1.5 (vertical) and a p-value < 0.05 (horizontal) (Wald test). The plots were generated from three independent replicates.

screen for mutants capable of bypassing the L1 arrest when CDK-12 is inhibited (Fig. 1A). We retrieved a mutation in the non-essential CTD-S5P phosphatase SSUP-72 that requires the PINN-1 isomerase to dephosphorylate the Pol II CTD (Fig. 1B–F). We analyzed the genome-wide effect of the loss of CDK-12 or SSUP-72 on transcription and found that SSUP-72 is implicated in the coordinated expression of genes organized in operons (Fig. 3).

We used the GRO-seq method to determine the effect of CDK-12 inactivation genome-wide and found that the affects the overall occupancy of Pol II on lone genes, which represent 75% of all genes (Fig. 2A). It has previously been reported that the Pol II elongation rate increases during mammalian transcription[38]. In *C. elegans*, Pol II undergoes very moderate 5′ pausing and extensive 3′ pausing[39], both being reduced upon CDK-12 loss (Fig. 2A). Our data suggest that CDK-12 enhances Pol II processivity as it transitions from initiation to elongation and slows it down at the transition from elongation to termination. Remarkably, slower Pol II in CDK-12 mutants itself does not negatively impact growth nor development, as the suppressor strain grows comparably to wild type, despite showing a Pol II profile that resembles that of CDK-12 mutants. In agreement with the notion that slow Pol II has little effect on transcription, steady-state mRNA levels of lone genes are largely unaffected upon CDK-12as inhibition (Fig. 2B). Therefore, altered Pol II processivity in CDK-12 mutants does not drastically alter transcriptome composition.

In *C. elegans*, the SL2 snRNP is recruited to transcribed operons by the CtsF complex[23]. We have previously reported that CDK-12-dependent CTD S2P is required for efficient CstF occupancy and SL2 *trans-splicing*. The unprotected 5′ ends resulting from inefficient SL2 *trans-splicing* in CDK-12 mutants result in mRNA degradation by exonucleases and intra-operons torpedo termination[18]. We report here that the loss of SSUP-72 CTD S5P phosphatase activity or any down-regulation of the SSUP-72/PINN-1 module compensates for CDK-12 inactivation (Fig. 1). We propose a model where SSUP-72 loss-of-function mutants alter Pol II residence time at 3′ ends. This affects pre-mRNA cleavage dynamics, which disfavors premature torpedo termination within operons (Fig. 4B). Consequently, the expression of growth and developmental genes reaches a level sufficient to prevent the L1 arrest in the *cdk-12as;ssup-72(lf)* double mutants. It is possible that the decreased expression of a single gene or a subset of genes belonging to the same pathway results in the early developmental arrest observed in CDK-12 loss-of-function mutants. Our preliminary observation that treatment with the JNK inhibitor *SP600125* is capable of suppressing the effects of CDK-12as inhibition may support this possibility and will be the topic of further investigations.

Yeast Ssu72 was initially discovered as a part of the 3′ end processing machinery where it affects in the termination of non-polyA and some polyA RNAs[24]. In *C. elegans*, the inactivation of SSUP-72 leads to a specific read-through transcription of an early PAS within the *unc-44* gene and to antitermination, resulting in the expression of the long form of ankyrin[29,40,41]. Even though the mechanistic details may be different, we see this unique case as a proxy of operon transcription, where the genetic ablation of CTD S5P dephosphorylation counteracts early termination. Our data suggest that SSUP-72 controls Pol II speed on TES (Fig. 4C), which kinetically impacts 3′ processing events. For operons, slow 3′-end processing extends Pol II occupancy, safeguarding the RNA from exonuclease degradation, which gives time for *trans-splicing* to occur and averts premature torpedo termination. While this is crucial for operonic gene expression when CDK-12 is inhibited, it has minimal impact on non-operonic genes. We presume that the effects of eliminating the SSUP-72/PINN-1 module on termination are genetically buffered by cellular factors that collaborate with the CTD to promote robust and efficient termination. Eliminating the SSUP-72/PINN-1 module only results in anti-termination when an alternative pathway to termination is available, such as in the case of SL2 *trans-splicing* within operons.

In Drosophila and mammals, dephosphorylation of CTD S5P facilitates the recruitment of PCF11, which binds to CTD S2P and nascent RNA, ultimately disrupting the elongation complex[42–44]. Here, we show that the loss of the SSUP-72/PINN-1 module suppresses the inhibition of CDK-12as. A possible explanation for the suppression is that increased CTD S5P interferes with PCF-11 recruitment to transcribing Pol II, thereby stabilizing the elongation complex and preventing early termination. In accordance with this, PCF11 depletion in yeast, flies, and mammalian cells results in increased transcriptional readthrough[44–46].

This work provides new key insights on the role of CDK-12 and SSUP-72/PINN-1 during transcription and places them in the physiological context of post-embryonic development in *C. elegans*.

Methods

Resource availability

All materials including strains are maintained at the University of Namur and should be requested from the Lead contact, Damien Hermand (*Damien.Hermand@crick.ac.uk*).

Strains and maintenance

Worms were maintained at 20 °C on Nematode Growth Media (NGM)−agar plates [51.3 mM NaCl, 1 mM $CaCl_2$, 1 mM $MgSO_4$, 25 mM KH_2PO_4, cholesterol (5 μg/ml), and 1.25 g of peptone with 8.5 g of agar for 500 ml] seeded with *Escherichia coli* OP50. In liquid medium, they were cultured on a shaker at 20 °C in S-Basal [0.1 M NaCl, 50 mM KH_2PO_4, 3 mM $MgSO_4$, 4 mM $CaCl_2$, 1 mM potassium citrate, and cholesterol (5 μg/ml)] with *E. coli* HB101 as described in ref. 47. N_2 (Bristol strain) was used as a wild type. Some strains were provided by the CGC, which is funded by NIH Office of Research Infrastructure Programs (P40 OD010440). Others were obtained from the National BioResource Project (Mitani Lab) or the Jorgensen laboratory. A list of strains used in this study is included in the Supplementary Table 1. All genome edits in this study were performed as described in ref. 48. Briefly, crRNA (IDT), tracrRNA (IDT, 1072532), and Cas9 (IDT, 1081060) were assembled in vitro and delivered as an RNP. Repair templates were delivered as single-strand oligonucleotides (IDT, ultramer).

crRNAs, repair templates, and primers used to detect and sequence the edits are provided in Supplementary Table 2.

EMS mutagenesis suppressor screen

The screen for suppressors of the L1 arrest induced by the inhibition of CDK-12as was performed as described in refs. 49,50. Briefly, *CDK-12as* L4 worms were washed in M9 and incubated in 50 mM EMS for 4 h at 20 °C. Mutagenized worms were washed in M9 and left to recover at 20 °C on NGM plates seeded with OP50. Once the F1 offspring reached the L4 stage, worms were transferred to plates containing 2 μM of 3MB-PP1 and allowed to lay eggs. The F1 animals were discarded, and F2 eggs were allowed to grow for 96 h at 20°C. Worms that grew beyond the L1 arrest were selected and re-rested on a fresh plate containing 2 μM of 3MB-PP1. Worms whose progeny did not L1 arrest were kept. DNA was extracted and sequenced as described in ref. 50. Candidate suppressive mutations were identified as SNPs with >95% read ratio (alternative/reference) compared to the *CDK-12as* strain. The SnpEff tool[51] was used to predict the putative function, and only SNPs annotated as low putative impact were retained.

Analog inhibition assay

Inhibition was performed on NGM plates, supplemented with 3MB-PP1, which was added to the desired concentration before pouring. For the phenotypical suppression assay, L4 worms were picked onto plates containing the inhibitor, and their progeny was evaluated after 96 h. To measure the length, hypochlorite-synchronized L1s were dropped on plates containing the inhibitor and incubated for 72 h before measurements. The measurements were conducted as described in ref. 52.

Protein extraction and Western blots

Hypochlorite-synchronized L1 worms (~50,000) were grown in liquid culture for 4 h, collected, washed 3× in M9, and flash-frozen in liquid nitrogen in 50 μl in a 1.5 mL centrifuge tube. Frozen pellets were supplemented with 50 μL of lysis buffer composed of 20 mM HEPES (pH 7.5), 125 mM sodium citrate, 0.1% (v/v) Tween 20, 0.5% (v/v) Triton X-100, 2 mM MgCl2, 1 mM DTT, proteases inhibitors (Roche) and phosphatases Inhibitors (Roche). Zirconia beads (100 μL; 11079105Z Cole-Parmer) were added to the worm suspension and homogenized at 4 °C in a FastPrep-24 benchtop homogenizer (MP Biochemicals) for six cycles of 20 s at 6 m/s with a 2-min rest between each cycle. A hole was poked in the microcentrifuge tube, then was inserted into another 1.5 mL microcentrifuge tube and spun at 1000 × *g* for 2 min at 4 °C. Beads were washed with 50 μL of lysis buffer and spun again. The lysate collected in the bottom tube was centrifugated at 14,000 × *g* for 30 min at 4 °C, and the supernatant was transferred to clean tubes. For each blot, 16 μL of supernatant were stained with Cy5 total protein staining (RPN4000, Cytiva) according to manufacturer instructions. Extracts were loaded on Bio-Rad mini-PROTEAN TGX gel 4–15% and then transferred to a nitrocellulose membrane using the Bio-Rad Trans-Blot Turbo transfer system, set up for high−molecular weight proteins (1.3 A, up to 25 V). The membrane was then blocked in skim milk powder (5%, Sigma-Aldrich) for at least 1 h. Primary antibodies were incubated for 1 h (Anti−CTD S5P 4H8 1/1000 (abcam, ab5408), Anti−CTD S2P 3E10 1/1000 (Millipore, 04-1571)). The membranes were washed 3× in PBS-Tween (0.05%) and incubated 1 h with secondary antibodies (anti-mouse immunoglobulin G (IgG) Perox (1/2000; GE, NA931) and anti-rat IgG Perox (1/2000; Dako, P0450)) then washed 2× in PBS-T and 1x in PBS. PerkinElmer Western Lightning Plus-ECL (enhanced chemiluminescence) was used for ECL, and detection was performed on an Amersham™ ImageQuant 800 machine. Quantification was performed using proprietary Cytiva quantification software and normalized to total protein levels. Uncropped scans are provided in Supplementary Information.

RNA-sequencing

Hypochlorite-synchronized L1 worms (~100,000) were grown in liquid for 4 h in the presence or absence of 3MB-PP1 (2 μM; 529582-5MG Sigma-Alderich), collected, washed 3× in M9, resuspended in 1 mL TRIzol™ reagent (Invitrogen #15596026) in 2 mL microcentrifuge tube and flash frozen in liquid nitrogen. Zirconia (200 μL; 11079105Z Cole-Parmer) were added to thawed TRIzol and homogenized at 4 °C in a FastPrep-24 benchtop homogenizer (MP Biochemicals) for six cycles of 20 s at 6 m/s with a 2-min rest between each cycle. To the lysate was added 100 μL of 1-Bromo-3-chloropopane (BCP; Sigma #B9674), mixed by vortexing, incubated at RT for 15 min, and centrifuged at 12,000 × *g* for 15 min. The upper aqueous phase (~450 μL) was transferred to an RNAse-free low-binding microcentrifuge tube, supplemented with 2 μL GlycoBlue and 500 μL isopropanol, mixed well and incubated at RT for 15 min to precipitate RNA. The RNA was then pelleted by centrifugation at 12,000 × *g* for 15 min at 4 °C. The pellet was then washed 1× in 75% ice-cold ethanol, air-dried, and resuspended in nuclease-free water. Concentration was assessed by QuBit and RNA integrity with BioAnalyzer (Agilent). Only RNAs with RIN > 8 were kept for RNA-seq. DNAse treatment was performed using TurboDNAse (Ambion #AM2238) following manufacturer's instructions. Ribosomal and mitochondrial were removed using a custom depletion strategy (Sequalis). RNA-seq library preparation was made using the Illumina TruSeq stranded total RNA library preparation kit following the manufacturer's instructions.

Global run on sequencing

Hypochlorite-synchronized L1 worms (~400,000) were grown for 4 h in the presence of food and 3MB-PP1 (2 μM; 529582-5MG Sigma-Alderich), collected, washed 3× in M9, and flash frozen in liquid nitrogen in a 1.5 mL microcentrifuge tube. GRO-seq was performed as previously described[53] with modifications to the nuclei isolation protocol. Nuclei were isolated from L1s (~400,000) with a 7 mL metallic dounce, using 120 strokes. To remove debris, the lysate was slowly spun at 200 × *g* for 6 min at 4 °C, and the supernatant was carefully transferred to a new low-binding microcentrifuge tube. The supernatant was then pelleted at 1000 × *g* for 8 min at 4 °C, washed once in NEB buffer, and resuspended in 100 μL freezing buffer.

Bioinformatics analysis

For all high-throughput sequencing experiments, reads were mapped on the *C. elegans* genome version WBcel235 (ce11). RNA-seq reads were aligned using HISAT2 (2.1.0)[54] while GRO-seq and were aligned using Bowtie2 (2.5.4)[55]. BAM files were processed using the Samtools suite. Feature quantification was computed using FeatureCounts (2.0.3)[56]. All analyses and figure drawings were performed within the R (4.4.2) programming language in the RStudio environment. Differential expression analysis was performed with DESeq2 (1.46.0)[57]. Criteria for differential expression are a false discovery rate <0.01 and absolute fold change >1.5. Metagenes were computed using DeepTools (3.5.6)[58].

Statistics and reproducibility

Figures and illustrations were prepared using Inkscape (ver 1.4). Measurements were sampled from individual biological replicates. Micrographs for 3MB-PP1 assays were performed at least five times, and representative micrographs were displayed. RNA-seq experiments, GRO-seq, and Western blots were performed three times. Worm length measurements were performed twice, and data points were pulled together for visualization. The statistical tests used are specified in the corresponding figure legends. No statistical methods were used to predetermine the sample size.

Reporting summary

Further information on research design is available in the Nature Portfolio Reporting Summary linked to this article.

Data availability

GRO-seq and RNA-seq raw and processed data are available on GEO under the following accession numbers. GRO-seq GSE263769, RNA-seq of SSUP-72 mutants GSE263771, and RNA-seq of CDK-12as and SSUP-72 GSE263774. A source file containing Western blot quantifications and worm length measurements has been provided. Source data are provided with this paper.

References

1. Buratowski, S. Progression through the RNA polymerase II CTD cycle. *Mol. Cell* **36**, 541–546 (2009).
2. Perales, R. & Bentley, D. "Cotranscriptionality": the transcription elongation complex as a nexus for nuclear transactions. *Mol. Cell* **36**, 178–191 (2009).
3. Liu, P., Kenney, J. M., Stiller, J. W. & Greenleaf, A. L. Genetic organization, length conservation, and evolution of RNA polymerase II carboxyl-terminal domain. *Mol. Biol. Evol.* **27**, 2628–2641 (2010).
4. Zhou, Q., Li, T. & Price, D. H. RNA polymerase II elongation control. *Ann. Rev. Biochem.* **81**, 119–143 (2012).
5. Belotserkovskaya, R. & Reinberg, D. Facts about FACT and transcript elongation through chromatin. *Curr. Opin. Genet. Dev.* **14**, 139–146 (2004).
6. Chapman, R. D., Heidemann, M., Hintermair, C. & Eick, D. Molecular evolution of the RNA polymerase II CTD. *Trends Genet.* **24**, 289–296 (2008).
7. Liu, P., Greenleaf, A. L. & Stiller, J. W. The essential sequence elements required for RNAP II carboxyl-terminal domain function in yeast and their evolutionary conservation. *Mol. Biol. Evol.* **25**, 719–727 (2008).
8. Ho, C. K. & Shuman, S. Distinct roles for CTD Ser-2 and Ser-5 phosphorylation in the recruitment and allosteric activation of mammalian mRNA capping enzyme. *Mol. Cell* **3**, 405–411 (1999).
9. Meinhart, A., Kamenski, T., Hoeppner, S., Baumli, S. & Cramer, P. A structural perspective of CTD function. *Genes Dev.* **19**, 1401–1415 (2005).
10. Stiller, J. W. & Cook, M. S. Functional unit of the RNA polymerase II C-terminal domain lies within heptapeptide pairs. *Eukaryot. Cell* **3**, 735–740 (2004).
11. Schwer, B. & Shuman, S. Deciphering the RNA polymerase II CTD code in fission yeast. *Mol. Cell* **43**, 311–318 (2011).
12. Ahn, S. H., Kim, M. & Buratowski, S. Phosphorylation of serine 2 within the RNA polymerase II C-terminal domain couples transcription and 3′ end processing. *Mol. Cell* **13**, 67–76 (2004).
13. Gu, B., Eick, D. & Bensaude, O. CTD serine-2 plays a critical role in splicing and termination factor recruitment to RNA polymerase II in vivo. *Nucleic Acids Res.* **41**, 1591–1603 (2013).
14. Kim, M. et al. The yeast Rat1 exonuclease promotes transcription termination by RNA polymerase II. *Nature* **432**, 517–522 (2004).
15. Cassart, C., Drogat, J., Migeot, V. & Hermand, D. Distinct requirement of RNA polymerase II CTD phosphorylations in budding and fission yeast. *Transcription* **3**, 231–234 (2012).
16. Coudreuse, D. et al. A gene-specific requirement of RNA polymerase II CTD phosphorylation for sexual differentiation in S. pombe. *Curr. Biol.* **20**, 1053–1064 (2010).
17. Lee, J. M. & Greenleaf, A. L. CTD kinase large subunit is encoded by CTK1, a gene required for normal growth of Saccharomyces cerevisiae. *Gene Expr.* **1**, 149–167 (1991).
18. Cassart, C. et al. RNA polymerase II CTD S2P is dispensable for embryogenesis but mediates exit from developmental diapause in C. elegans. *Sci. Adv.* **6**, https://doi.org/10.1126/sciadv.abc1450 (2020).
19. Blumenthal, T., Davis, P. & Garrido-Lecca, A. Operon and non-operon gene clusters in the C. elegans genome. *WormBook*, 1–20. https://doi.org/10.1895/wormbook.1.175.1 (2015).
20. Blumenthal, T. & Gleason, K. S. Caenorhabditis elegans operons: form and function. *Nat. Rev. Genet.* **4**, 112–120 (2003).
21. Zaslaver, A., Baugh, L. R. & Sternberg, P. W. Metazoan operons accelerate recovery from growth-arrested states. *Cell* **145**, 981–992 (2011).
22. Blumenthal, T. et al. A global analysis of Caenorhabditis elegans operons. *Nature* **417**, 851–854 (2002).
23. Evans, D. et al. A complex containing CstF-64 and the SL2 snRNP connects mRNA 3′ end formation and trans-splicing in C. elegans operons. *Genes Dev.* **15**, 2562–2571 (2001).
24. Ganem, C. et al. Ssu72 is a phosphatase essential for transcription termination of snoRNAs and specific mRNAs in yeast. *EMBO J.* **22**, 1588–1598 (2003).
25. Meinhart, A., Silberzahn, T. & Cramer, P. The mRNA transcription/processing factor Ssu72 is a potential tyrosine phosphatase. *J. Biol. Chem.* **278**, 15917–15921 (2003).
26. Steinmetz, E. J. & Brow, D. A. Ssu72 protein mediates both poly(A)-coupled and poly(A)-independent termination of RNA polymerase II transcription. *Mol. Cell Biol.* **23**, 6339–6349 (2003).
27. Werner-Allen, J. W. et al. cis-Proline-mediated Ser(P)5 dephosphorylation by the RNA polymerase II C-terminal domain phosphatase Ssu72. *J. Biol. Chem.* **286**, 5717–5726 (2011).
28. Shim, E. Y., Walker, A. K., Shi, Y. & Blackwell, T. K. CDK-9/cyclin T (P-TEFb) is required in two postinitiation pathways for transcription in the C. elegans embryo. *Genes Dev.* **16**, 2135–2146 (2002).
29. LaBella, M. L. et al. Casein kinase 1delta stabilizes mature axons by inhibiting transcription termination of ankyrin. *Dev. Cell* **53**, 130 (2020).
30. Kim, H. S. et al. Functional interplay between Aurora B kinase and Ssu72 phosphatase regulates sister chromatid cohesion. *Nat. Commun.* **4**, 2631 (2013).
31. Park, E. J. et al. Ssu72 phosphatase is essential for thermogenic adaptation by regulating cytosolic translation. *Nat. Commun.* **14**, 1097 (2023).
32. Escandell, J. M. et al. Ssu72 phosphatase is a conserved telomere replication terminator. *EMBO J.* **38**, https://doi.org/10.15252/embj.2018100476 (2019).
33. Xiang, K. et al. Crystal structure of the human symplekin-Ssu72-CTD phosphopeptide complex. *Nature* **467**, 729–733 (2010).
34. Jeronimo, C., Collin, P. & Robert, F. The RNA polymerase II CTD: the increasing complexity of a low-complexity protein domain. *J. Mol. Biol.* **428**, 2607–2622 (2016).
35. Tellier, M. et al. CDK12 globally stimulates RNA polymerase II transcription elongation and carboxyl-terminal domain phosphorylation. *Nucleic Acids Res.* **48**, 7712–7727 (2020).
36. Gromak, N., West, S. & Proudfoot, N. J. Pause sites promote transcriptional termination of mammalian RNA polymerase II. *Mol. Cell Biol.* **26**, 3986–3996 (2006).
37. Yague-Sanz, C. & Hermand, D. SL-quant: a fast and flexible pipeline to quantify spliced leader trans-splicing events from RNA-seq data. *Gigascience* **7**. https://doi.org/10.1093/gigascience/giy084 (2018).
38. Krajewska, M. et al. CDK12 loss in cancer cells affects DNA damage response genes through premature cleavage and polyadenylation. *Nat. Commun.* **10**, 1757 (2019).
39. Baugh, L. R., Demodena, J. & Sternberg, P. W. RNA Pol II accumulates at promoters of growth genes during developmental arrest. *Science* **324**, 92–94 (2009).
40. Chen, F., Chisholm, A. D. & Jin, Y. Tissue-specific regulation of alternative polyadenylation represses expression of a neuronal ankyrin isoform in C. elegans epidermal development. *Development* **144**, 698–707 (2017).
41. Chen, F. et al. Context-dependent modulation of Pol II CTD phosphatase SSUP-72 regulates alternative polyadenylation in neuronal development. *Genes Dev.* **29**, 2377–2390 (2015).

42. Licatalosi, D. D. et al. Functional interaction of yeast pre-mRNA 3′ end processing factors with RNA polymerase II. *Mol. Cell* **9**, 1101–1111 (2002).
43. Meinhart, A. & Cramer, P. Recognition of RNA polymerase II carboxy-terminal domain by 3′-RNA-processing factors. *Nature* **430**, 223–226 (2004).
44. Zhang, Z. & Gilmour, D. S. Pcf11 is a termination factor in Drosophila that dismantles the elongation complex by bridging the CTD of RNA polymerase II to the nascent transcript. *Mol. Cell* **21**, 65–74 (2006).
45. West, S. & Proudfoot, N. J. Human Pcf11 enhances degradation of RNA polymerase II-associated nascent RNA and transcriptional termination. *Nucleic Acids Res.* **36**, 905–914 (2008).
46. Baejen, C. et al. Genome-wide analysis of RNA polymerase II Termination at protein-coding genes. *Mol. Cell* **66**, 38–49.e36 (2017).
47. Hibshman, J. D., Webster, A. K. & Baugh, L. R. Liquid-culture protocols for synchronous starvation, growth, dauer formation, and dietary restriction of Caenorhabditis elegans. *STAR Protoc.* **2**, 100276 (2021).
48. Ghanta, K. S., Ishidate, T. & Mello, C. C. Microinjection for precision genome editing in Caenorhabditis elegans. *STAR Protoc.* **2**, 100748 (2021).
49. Jorgensen, E. M. & Mango, S. E. The art and design of genetic screens: caenorhabditis elegans. *Nat. Rev. Genet.* **3**, 356–369 (2002).
50. Delaney, K., Strobino, M., Wenda, J. M., Pankowski, A. & Steiner, F. A. H3.3K27M-induced chromatin changes drive ectopic replication through misregulation of the JNK pathway in C. elegans. *Nat. Commun.* **10**, 2529 (2019).
51. Cingolani, P. et al. A program for annotating and predicting the effects of single nucleotide polymorphisms, SnpEff: SNPs in the genome of Drosophila melanogaster strain w1118; iso-2; iso-3. *Fly* **6**, 80–92 (2012).
52. Schoenauen, L., Stubbe, F. X., Van Gestel, D., Penninckx, S. & Heuskin, A. C. C. elegans: a potent model for high-throughput screening experiments investigating the FLASH effect. *Clin. Transl. Radiat. Oncol.* **45**, 100712 (2024).
53. Quarato, P. & Cecere, G. Global run-on sequencing to measure nascent transcription in C. elegans. *STAR Protoc.* **2**, 100991 (2021).
54. Salzberg, S. L. Next-generation genome annotation: we still struggle to get it right. *Genome Biol.* **20**, 92 (2019).
55. Langmead, B. & Salzberg, S. L. Fast gapped-read alignment with Bowtie 2. *Nat.Methods* **9**, 357–359 (2012).
56. Liao, Y., Smyth, G. K. & Shi, W. featureCounts: an efficient general purpose program for assigning sequence reads to genomic features. *Bioinformatics* **30**, 923–930 (2014).
57. Love, M. I., Huber, W. & Anders, S. Moderated estimation of fold change and dispersion for RNA-seq data with DESeq2. *Genome Biol.* **15**, 550 (2014).
58. Ramirez, F., Dundar, F., Diehl, S., Gruning, B. A. & Manke, T. deepTools: a flexible platform for exploring deep-sequencing data. *Nucleic Acids Res.* **42**, W187–W191 (2014).

Acknowledgements

We are grateful to Germano Cecere for help with GRO-seq, Sevinc Ercan for discussions, and Erik Jorgensen for strains. We thank Carlo Yague-Sanz for the discussions, Craig Mello, and François Bachand for comments on the manuscript. This work was supported by grants EMBO STF 8101, FNRS T.0012.14, FNRS J.0066.16, FNRS T.0112.21, and FNRS U.N032.22 to D.H. F.-X.S. was a FRIA Research fellow. P.P. is a FNRS Research fellow. D.H. worked at the University of Namur until November 2023 and is an honorary FNRS Director of Research.

Author contributions

F.-X.S. and D.H. designed the project. F.-X. S. designed, performed, and analyzed the experiments and data. P.P. helped to maintain and grow worms. F.S. contributed to the design of the EMS suppressor screen and performed it with D.H. at the University of Geneva. D.H. acquired funding and supervised the project. F.-X. S. and D.H. wrote the paper with inputs from other authors.

Competing interests

The authors declare no competing interests.

Additional information

Supplementary information The online version contains supplementary material available at https://doi.org/10.1038/s41467-025-57847-x.

Correspondence and requests for materials should be addressed to Damien Hermand.

Peer review information *Nature Communications* thanks John Hanover and the other, anonymous, reviewer(s) for their contribution to the peer review of this work. A peer review file is available.